



## Practice of Epidemiology

# Characterizing and Comparing the Seasonality of Influenza-Like Illnesses and Invasive Pneumococcal Diseases Using Seasonal Waveforms

Matthieu Domenech de Cellès\*, Hélène Arduin, Emmanuelle Varon, Cécile Souty, Pierre-Yves Boëlle, Daniel Lévy-Bruhl, Sylvie van der Werf, Jean-Claude Souly, Didier Guillemot, Laurence Watier, and Lulla Opatowski

\* Correspondence to Dr. Matthieu Domenech de Cellès; Biostatistics, Biomathematics, Pharmacoepidemiology and Infectious Diseases (B2PHI), Institut Pasteur, 25 rue du Dr Roux, 75015 Paris, FRANCE (e-mail: matthieu.domenech-de-celles@pasteur.fr).

Initially submitted May 15, 2017; accepted for publication October 6, 2017.

The seasonalities of influenza-like illnesses (ILIs) and invasive pneumococcal diseases (IPDs) remain incompletely understood. Experimental evidence indicates that influenza-virus infection predisposes to pneumococcal disease, so that a correspondence in the seasonal patterns of ILIs and IPDs might exist at the population level. We developed a method to characterize seasonality by means of easily interpretable summary statistics of seasonal shape—or seasonal waveforms. Nonlinear mixed-effects models were used to estimate those waveforms based on weekly case reports of ILIs and IPDs in 5 regions spanning continental France from July 2000 to June 2014. We found high variability of ILI seasonality, with marked fluctuations of peak amplitudes and peak times, but a more conserved epidemic duration. In contrast, IPD seasonality was best modeled by a markedly regular seasonal baseline, punctuated by 2 winter peaks in late December to early January and January to February. Comparing ILI and IPD seasonal waveforms, we found indication of a small, positive correlation. Direct models regressing IPDs on ILIs provided comparable results, even though they estimated moderately larger associations. The method proposed is broadly applicable to diseases with unambiguous seasonality and is well-suited to analyze spatially or temporally grouped data, which are common in epidemiology.

infectious disease seasonality; influenza; influenza-like illnesses; invasive pneumococcal diseases; mixed-effects models; pneumococcus; seasonal waveforms

Abbreviations: BIC, Bayesian information criterion; ILI, influenza-like illness; IPD, invasive pneumococcal disease; SD, standard deviation.

Seasonality is a striking feature of many infectious diseases in humans (1–3). These include infections caused by influenza viruses, a major cause of morbidity and mortality worldwide (4), and by *Streptococcus pneumoniae* (the pneumococcus), a commensal bacterium of the nasopharynx responsible for a wide spectrum of conditions ranging from mild upper respiratory tract infections to severe invasive pneumococcal diseases (IPDs) (5, 6). IPDs exhibit remarkably consistent seasonal fluctuations across climatically diverse locations, with a gradual increase of cases from autumn to a winter peak, followed by a decline to a summer nadir (7–15). Influenza activity—usually quantified via syndromic surveillance of influenza-like illnesses (ILIs)—displays even more pronounced seasonality in temperate regions, with epidemics peaking during winter and

lasting 10–15 weeks (14, 16–18). Previous work has explored the potential causes of such patterns (e.g., seasonal changes in host disease susceptibility (7, 19), host behavior (19, 20), or pathogen survival outside the host (21, 22)). However, the relative contributions of these mechanisms (or others) have not yet been fully elucidated (23, 24).

*S. pneumoniae* interaction with cocirculating pathogens may also contribute to the seasonality of IPDs. Indeed, it has long been posited that influenza infection facilitates pneumococcal disease (25), a hypothesis supported by recent experimental evidence in animal models (26, 27). In contrast, the evidence garnered from population-level studies has been less consistent (8, 10, 11, 14, 28–31), perhaps because of heterogeneity of methods or data collection in different studies. With

application of common statistical techniques across diverse settings, large-scale comparative studies are essential to document and generate hypotheses about the seasonality of ILIs and IPDs. Yet such studies remain scarce (14), and further investigations are warranted.

We examined highly resolved ILI and IPD incidence data in France, spanning 14 years and 5 geographical regions. We developed a novel method to estimate summary statistics of seasonal shape via nonlinear mixed-effects models. We have shown this method to be a useful and practical quantitative tool to characterize and compare ILI and IPD seasonalities.

## METHODS

### Data

**ILI data.** ILI incidence data were available from the French *Sentinelles* network, a nationwide surveillance system described elsewhere (32, 33). Briefly, a sample of general practitioners across France report weekly numbers of ILI cases, defined clinically as sudden onset of fever ( $\geq 39^\circ\text{C}$ ), associated with myalgia and respiratory symptoms (e.g., cough and sore throat). Weekly ILI incidences were estimated by multiplying the mean number of reported cases per participating general practitioner by the total number of general practitioners in the area (34). These data have been used extensively to investigate the spatiotemporal dynamics of influenza in France (20, 34–36). During the study period, broad information on influenza types and subtypes circulating in France was available, but type-specific weekly time series could not be constructed (see Web Appendix 1 and Web Table 1, available at <https://academic.oup.com/aje>). For this analysis, we aggregated the data into 5 geographical regions spanning continental France: Île-de-France (including Paris), Northwest, Northeast, Southeast, and Southwest. For each region, we constructed weekly time series of ILIs during epidemiologic years 2000/2001–2013/2014 (14 seasons and 730 weeks overall (Figure 1 and Web Figure 1 in Web Appendix 1)), where an epidemiologic year  $n/n + 1$  consisted of all weeks between week 27 (the first week of July) of calendar year  $n$  and week 26 of calendar year  $n + 1$ .

**IPD data.** IPD incidence data were available from the *Epi-bac* network, a nationwide, hospital-based surveillance system that has tracked trends of IPDs (37, 38) for over 2 decades. The participating hospital laboratories are distributed homogeneously throughout France and cover >70% of the French population. An IPD case was defined as the isolation of *S. pneumoniae* or the detection of pneumococcal DNA in cerebrospinal fluid (meningitis) or blood (nonmeningitis bacteremia). As we did for the ILI data, we constructed weekly time series of cases during 2000/2001–2013/2014 for the 5 geographical regions of France (Figure 2 and Web Figure 2).

**Demographic data.** Yearly estimates of population sizes in every region were available from the French National Institute of Statistics and Economic Studies (39). Summary demographic characteristics for every region are presented in Web Table 2.

### Empirical models of ILI and IPD seasonalities

**ILI model.** As shown in Figure 1 and Web Figure 1, ILI dynamics were markedly epidemic, with a definite peak and

most cases concentrated around that peak every year. To analyze ILI seasonality, we fitted an empirical model approximating the epidemic curve of the susceptible-infected-recovered model for diseases with a low basic reproduction number (see Web Appendix 2, Keeling and Rohani (40), and Kermack and McKendrick (41)):

$$x_t = 10^{-2}N_t \frac{A}{\cosh^2 \frac{t-\phi}{\sigma}},$$

where  $x_t$  represents the weekly number of ILIs during week  $t$  and  $N_t$  is the population size at week  $t$ . The week number  $t$  was defined according to the International Organization for Standardization (ISO) 8601 format: weeks started on Mondays, and the week containing January 1 was considered week 1 if it had  $\geq 4$  days in the new year (and the last week of the previous year (week 52 or 53) otherwise). To avoid discontinuities, we centered the week number on the last week of calendar year  $n$  for each epidemiologic year  $n/n + 1$ . Therefore, week 0 is the last week of calendar year  $n$  and week 1 the first week of calendar year  $n + 1$ , and  $t = -25, \dots, 0, 1, \dots, 26$  for epidemiologic years counting 52 weeks. In the formula,  $A$  represents the peak amplitude (measured, via the scaling factor  $10^{-2}N_t$ , in cases per week per 100 population),  $\phi$  the peak week, and  $\sigma$  the peak width (in weeks). Because they shape ILI seasonality, those parameters are referred to as seasonal waveforms (10). In Web Appendix 2, we demonstrate that the total annual number of cases (or attack rate) is given by  $2A\sigma$  and that approximately 95% of cases occur during a time period of  $3.7\sigma$  weeks, which we define as the epidemic duration. The estimates of these 2 parameters are reported below, in addition to the other parameters.

**IPD model.** As shown in Figure 2 and Web Figure 2, IPD seasonality was almost constant, with regular variations during most of the year, interspersed by a marked peak at the end of each calendar year (week 0), another peak at the beginning of the year (weeks 1–10), and smaller peaks in autumn and in spring. Based on those observations, we represented IPD seasonality as the sum of a seasonal baseline modeled by a sine wave, and peaks modeled by the function used for the ILI data (Web Appendix 3):

$$x_t = \begin{cases} 10^{-5}N_t\mu \left( 1 + A_0 \cos \frac{2\pi(t-\phi_0)}{n_w} \right), & \text{if } n_p = 0 \\ 10^{-5}N_t \left[ \mu \left( 1 + A_0 \cos \frac{2\pi(t-\phi_0)}{n_w} \right) + \sum_{p=1}^{n_p} \frac{A_p}{\cosh^2 \frac{t-\phi_p}{\sigma_p}} \right], & \text{if } n_p \geq 1 \end{cases},$$

where  $t$  is the week number,  $x_t$  is the number of IPDs during week  $t$ ,  $N_t$  is the population size at week  $t$ ,  $n_w \in \{52, 53\}$  is the number of weeks in the epidemiologic year associated with week  $t$ , and  $n_p$  is the number of peaks. Here, the first term of the sum represents the seasonal baseline, with  $\mu$  being the average number of cases (measured, via the scaling

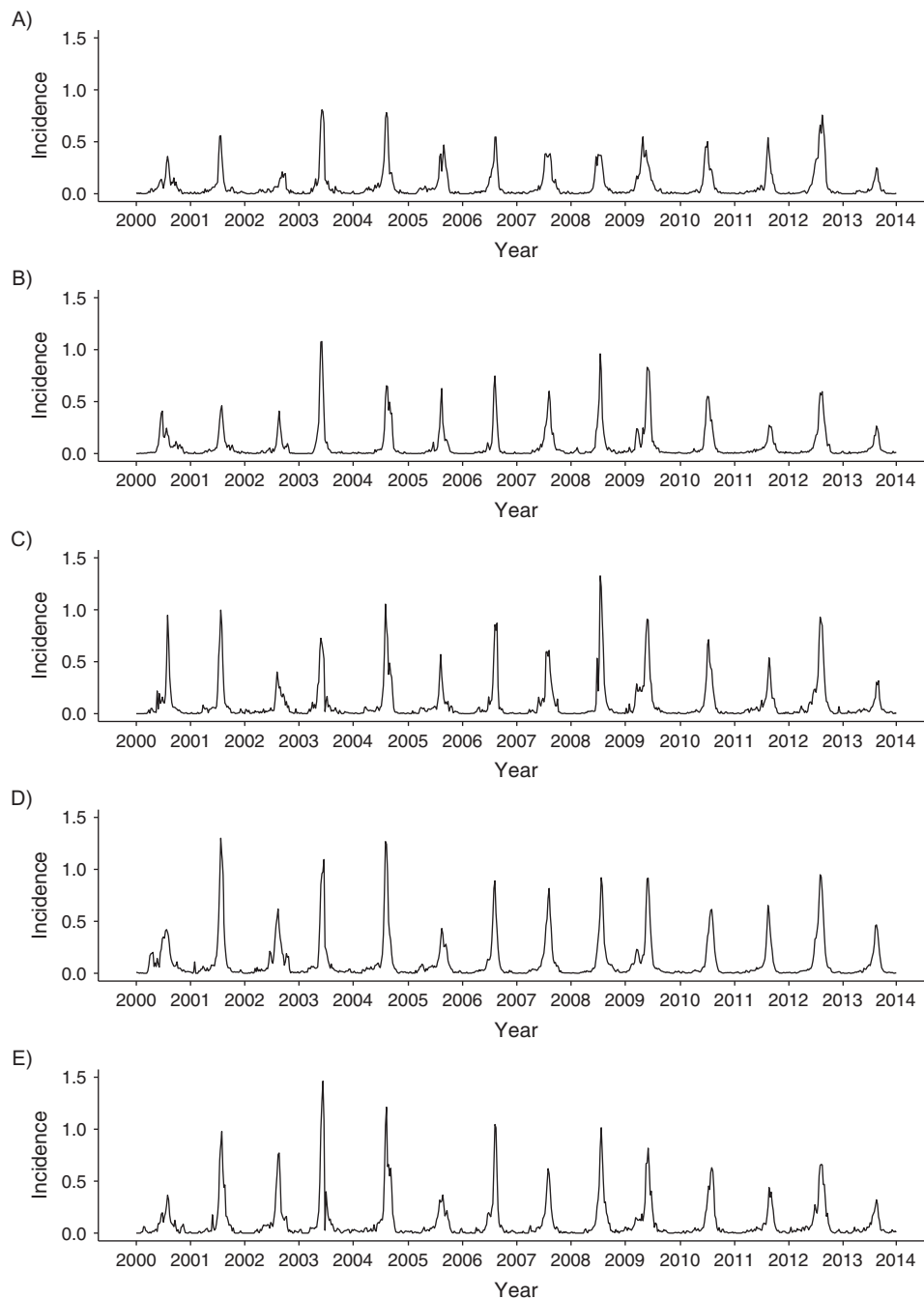


**Figure 1.** Influenza-like illness (ILI) incidence data in France, 2000–2014. Time series of ILI incidence (weekly cases per 100 population) in 5 regions spanning continental France. A) Île-de-France region; B) Northwest region; C) Northeast region; D) Southeast region; E) Southwest region. The x-axis ticks, placed at week 27 for years 2000–2013 and at week 26 for year 2014, delimit each epidemiologic year.

factor  $10^{-5}N_p$ , in cases per week per 100,000 population),  $A_0$  the semi-amplitude (relative to the average  $\mu$ ), and  $\phi_0$  the peak week. By analogy with the ILI model, the  $n_p$  IPD peaks are summarized by the waveforms  $A_p$  (peak amplitude, cases per week per 100,000 population),  $\phi_p$  (peak week), and  $\sigma_p$  (peak width, in weeks). We also define  $n_w\mu$  as the baseline annual cases (per 100,000 population),  $2A_p\sigma_p$  as the excess

of annual cases (per 100,000 population) due to peak  $p$ , and  $2A_p\sigma_p/(n_w\mu)$  as the relative (to the seasonal baseline) excess of annual cases due to peak  $p$ . In keeping with our central goal of comparing ILI and IPD seasonalities, we only tested models with  $n_p \leq 2$  peaks, constrained to occur during the period of ILI activity ( $t \in [-5, 15]$ , see Figure 1 and Web Figure 1).

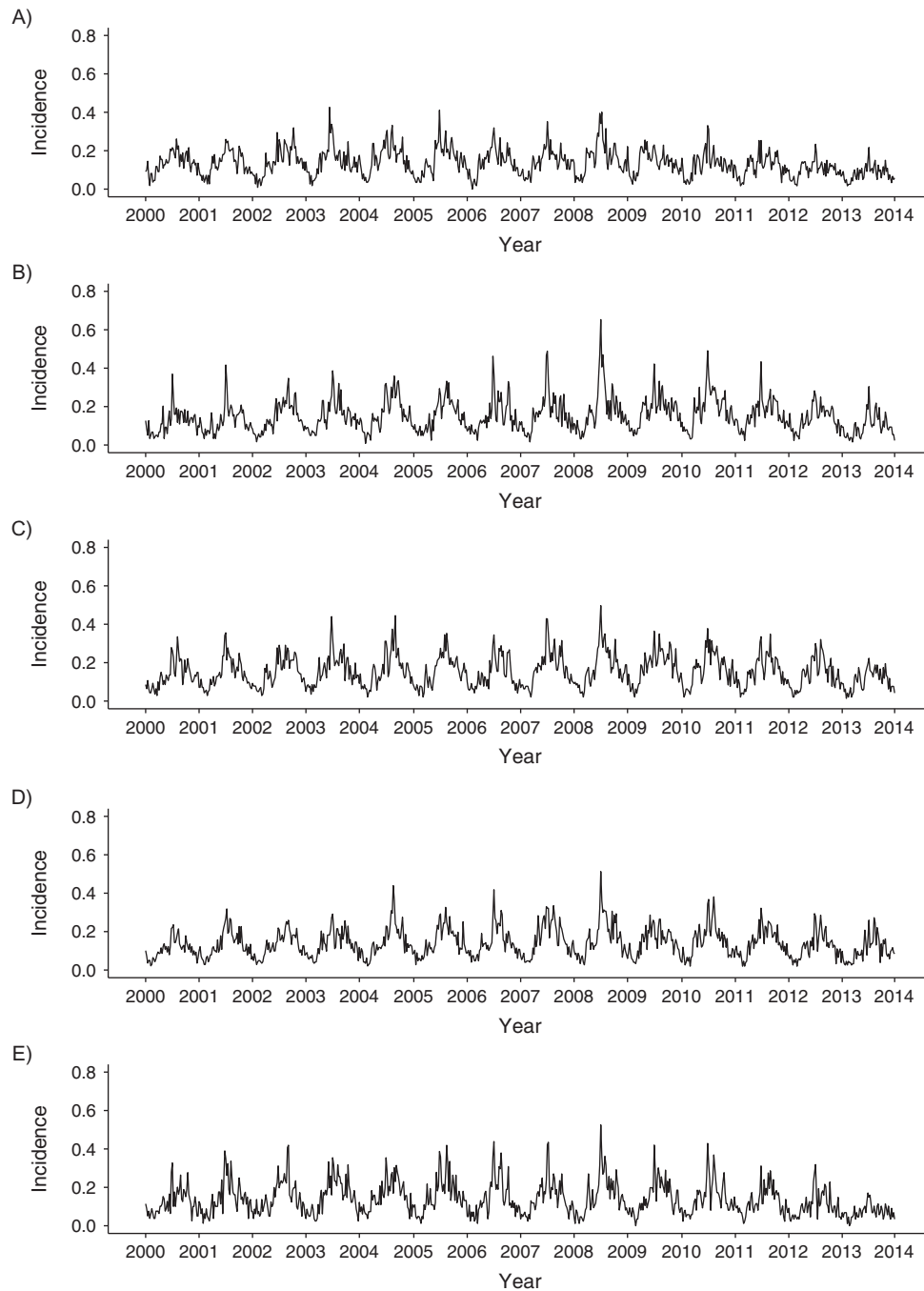


**Figure 2.** Invasive pneumococcal disease (IPD) incidence data in France, 2000–2014. Time series of IPD incidence (weekly cases per 100,000 population) in 5 regions spanning continental France. A) Île-de-France region; B) Northwest region; C) Northeast region; D) Southeast region; E) Southwest region. The x-axis ticks, placed at week 27 for years 2000–2013 and at week 26 for year 2014, delimit each epidemiologic year.

### Models estimation

To take into account the grouped (by region and by year) structure of ILI and IPD data, we fitted variants of the nonlinear models that incorporated both fixed effects and random effects—that is, nonlinear mixed-effects models (42). Let  $x_{it}$  represent the number of ILIs or IPDs during week  $t$  in

region-year  $i$  and  $f(t; \boldsymbol{\theta}_i)$  the nonlinear function modeling ILI or IPD dynamics, where  $\boldsymbol{\theta}$  is the vector of model parameters. We fitted models of the form:

$$\begin{aligned} x_{it} &= f(t; \boldsymbol{\theta}_i) + \epsilon_{it} \\ \boldsymbol{\theta}_i &= \boldsymbol{\beta} + \mathbf{b}_i \end{aligned}$$

where  $\beta$  is the vector of fixed effects,  $b_i \sim N(0, \Psi)$  the vector of random effects in region-year  $i$ , and  $\varepsilon_{it} \sim N(0, \sigma^2)$  is the within-group error. The estimation was completed in several steps according to the model building method presented in Pinheiro and Bates (42), from individual nonlinear least-squares estimations in each region-year to the estimation of the final nonlinear mixed-effects model. The parsimony of competing models was quantified using the Bayesian information criterion (BIC). Complete details of the estimation procedure are presented in Web Appendices 2 and 3. All estimations were performed using the nlme package (43), operating in R (R Foundation for Statistical Computing, Vienna, Austria) (44). Data and codes reproducing the analysis of the ILI data are provided as a supplement.

### Association between ILIs and IPDs

**Comparison of ILI and IPD seasonal waveforms.** To compare ILI and IPD seasonalities, we calculated Spearman correlation coefficients to quantify the association between their estimated seasonal waveforms. The waveforms considered were the peak week  $\phi$  and the total annual cases (ILI model), or total annual excess cases (IPD model),  $E = 2A\sigma$ . For each waveform, we calculated confidence intervals for the correlation coefficient by using a block bootstrap (with  $10^4$  bootstrap samples), where a block was defined as an epidemiologic year.

**Comparison with a direct regression model with ILIs.** We sought to compare the association estimated by the seasonal waveforms comparison with that estimated by direct regression models, the method most commonly employed in the literature (8, 11, 14, 29, 31) (but see also other methods, such as cross-correlation on pre-whitened data (28) or detection and comparison of outbreak periods (30)). To do so, we fitted a mixed-effects model that incorporated a seasonal baseline (sine wave) and ILIs directly as a covariate. For each region-year, we also calculated the relative (to the seasonal baseline) excess of IPD cases associated with ILIs (Web Appendix 4).

## RESULTS

### ILI seasonality

A total of 41,580,638 ILI cases were extrapolated from *Sentinelles* reports during the study period (Île-de-France, 6,481,491; Northwest, 6,879,606; Northeast, 10,057,549; Southeast, 11,920,277; Southwest, 6,241,715). During the 14 epidemic seasons, the dominant types or subtypes of influenza were A(H3N2) ( $n = 6$  seasons, Web Table 1), B ( $n = 3$ ), A(H1N1)pdm09 ( $n = 3$ ), and A(H1N1) ( $n = 2$ ); 5 epidemics were codominated by another type or subtype (2 with B and 1 each with A(H3N2), A(H1N1), or A(H1N1)pdm09). The region-year estimates of the seasonal waveforms  $\hat{\beta} + \hat{b}_i$  ( $\hat{\beta}$ , the vector of estimated fixed-effects;  $\hat{b}_i$ , the vector of estimated random-effects in region-year  $i$ ) are shown in Figure 3. To further quantify the random-effects variability across groups, we also report the random-effects standard deviation (SD, extracted from the diagonal entries in the variance-covariance matrix  $\Psi$ ) and the variation ratio (random-effects SD/fixed-effect) when discussing the seasonal waveforms below. The peak amplitude  $A$  displayed substantial variability across years and regions (fixed-effects

estimate 0.65, random-effects SD 0.29 weekly cases per 100; variation ratio 0.44), with a 7.6 factor variation in individual group estimates. The peak time  $\phi$  also varied across years (fixed effects ranging from week  $-4.9$  to week 8.2); except for 2 years with early epidemics (2003/2004 and 2009/2010), the peak occurred during weeks 0–10. By contrast, the peak time varied little from one region to another every year: After the first peak had occurred in a given region, the peaks in the other regions followed within an average of 2.0 weeks (ranging from 0.7 weeks during year 2012/2013 to 4.1 weeks during year 2000/2001), with no obvious spatial pattern of ILI spread. Compared with the peak amplitude and peak time, the peak width  $\sigma$  was more regular, averaging 3.4 weeks (random-effects SD 0.9 weeks; variation ratio 0.26), corresponding to an average 12.5-week epidemic duration (random-effects SD 3.3 weeks), with individual estimates ranging from 6.5 weeks (Northeast–2000/2001) to 21.4 weeks (Southeast–2000/2001). The total number of annual cases, or attack rate, averaged 4.4%, with marked year-to-year and region-to-region fluctuations (range, 1.5% in Île-de-France in 2013/2014 to 6.8% in the Southwest in 2004/2005). The inclusion of fixed differences between regions did not improve model parsimony for any waveform (Web Table 3).

Visual examination of the model fit showed good agreement with the ILI data, even though the model could not reproduce double peaks that occurred in a few region-years (e.g., Île-de-France in 2005/2006, Île-de-France in 2009/2010, Northwest in 2000/2001, and Southeast in 2000/2001) (Web Figure 3).

### IPD seasonality

A total of 64,542 IPD cases occurred during the study period (Île-de-France, 11,377; Northwest, 13,661; Northeast, 15,963; Southeast, 15,065; Southwest, 8,476). Comparing the parsimony of models with 0, 1, or 2 winter peaks (Web Table 4), the 1-peak model outperformed the model with no winter peak ( $\Delta\text{BIC} \approx -748$ ); the 2-peak model provided a more parsimonious fit than the 1-peak model, although the difference was smaller ( $\Delta\text{BIC} \approx -54$ ). We discuss the estimates of the 2-peak model below, and we also present those of the 1-peak model in Web Appendix 3 (Web Figures 4–6). The 2-peak model estimates for every region-year are shown in Figure 4. The final model did not include fixed differences between regions or between years for any waveform (Web Tables 5–6). The baseline average weekly cases (fixed-effect  $\mu = 0.13$ , random-effects SD 0.02 cases per week per 100,000 population; variation ratio 0.15) and the total baseline annual cases (fixed-effect  $n_{\text{y}}\mu = 7.0$ , random-effects SD 1.1 cases per year per 100,000) exhibited little variability between regions but higher variability between years. These year-to-year variations mirrored previously reported trends of pneumococcal meningitis in France (45, 46), marked by an initial increase after the introduction of the 7-valent pneumococcal conjugate vaccine in 2003, followed by a decline after the introduction of the 13-valent conjugate vaccine in 2010. In contrast, the relative amplitude (fixed-effect  $A_0 = 0.49$ ; no random effects) and the peak week (fixed-effect  $\phi_0 = 6.2$ , random-effects SD 1.4 weeks) of the seasonal baseline were very stable across years and regions.

According to the final 2-peak model, a first peak was located near the last week of every calendar year (fixed-effect  $\phi_1 = 0.5$ , random-effects SD 0.4 weeks), with substantial variations



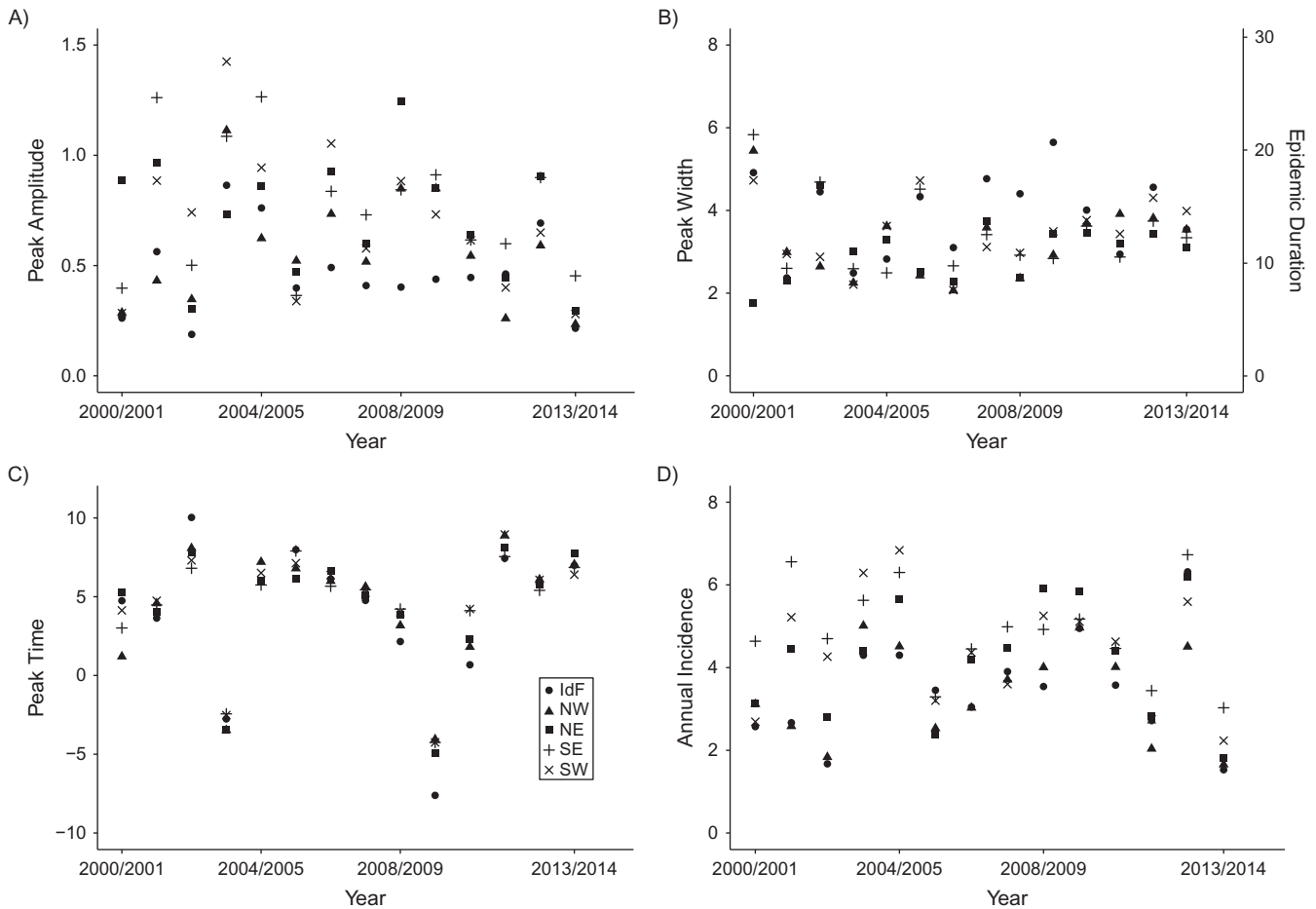


**Figure 3.** Influenza-like illness (ILI) seasonal waveforms, France, 2000–2014. The parameter estimates are presented every year (x-axis) in every region (symbol). The y-axis values differ for each panel. A) Peak amplitude ( $A$ , cases per week per 100); B) peak width ( $\sigma$ , weeks)/epidemic duration ( $3.7\sigma$ , weeks); C) peak time ( $\phi$ , week); D) annual incidence ( $2A\sigma$ , cases per year per 100). Abbreviations: IdF, Île-de-France; NW, Northwest; NE, Northeast; SE, Southeast; SW, Southwest.

of amplitude (fixed-effect  $A_1 = 0.16$ , random-effects SD 0.08 cases per week per 100,000; variation ratio 0.50) but not of width (fixed-effect  $\sigma_1 = 1.0$  week, no random-effects). The resulting relative excess of annual cases compared with baseline was 4.8% and ranged from 1.4% (Île-de-France in 2009/2010) to 9.8% (Northwest in 2008/2009).

Compared with peak 1, winter peak 2 had greater time variability (fixed-effect  $\phi_2 = 6.4$ , random-effects SD 1.4 weeks). Overall, that peak presence was less stable and less marked than the first peak, causing an average relative excess of annual cases of 2.2% (range, 1.4% in Île-de-France in 2007/2008 to 5.4% in the Southeast in 2004/2005). Therefore, peak 2 was marked only in a few region-years but negligible in most others.

Visual inspection of the model fit showed adequate agreement with the IPD data, even though the model slightly overestimated the summer IPD troughs (Web Figures 7 and 8).

### ILI-IPD association

Estimated correlations between ILI and IPD seasonal waveforms are given in Table 1. As expected from the tightly

constrained time of IPD peak 1 and the more variable peak time of ILIs, we found no peak 1–ILI association. Considering the whole study period (including years 2003/2004 and 2009/2010 with early ILI peaks; see Figure 3), an association was suggested with IPD peak 2. This association was more pronounced when restricting analysis to years with ILI peak time during the typical period of ILI activity (weeks 0–10), with evidence of a small, positive correlation between peak times and between total excess cases. With this restriction, the results also indicated a short, approximately 1-week lag between the IPD peak 2 and the ILI peak times.

The results of the direct regression model (Web Table 7 and Web Figure 9) indicated a short-term (0–1 week difference between IPD and ILI peaks), variable but overall small (median relative excess cases, 4.9%; median absolute deviation, 2.4%) association between ILIs and IPDs, except in a few region-years (relative excess cases exceeding 10% in Île-de-France in 2003/2004, Île-de-France in 2009/2010, and the Southeast in 2004/2005). Furthermore, the excess cases associated with ILIs in that model and with IPD peak 2 in the 2-peak model were markedly correlated (Spearman correlation coefficient 0.63 (95% CI: 0.48,

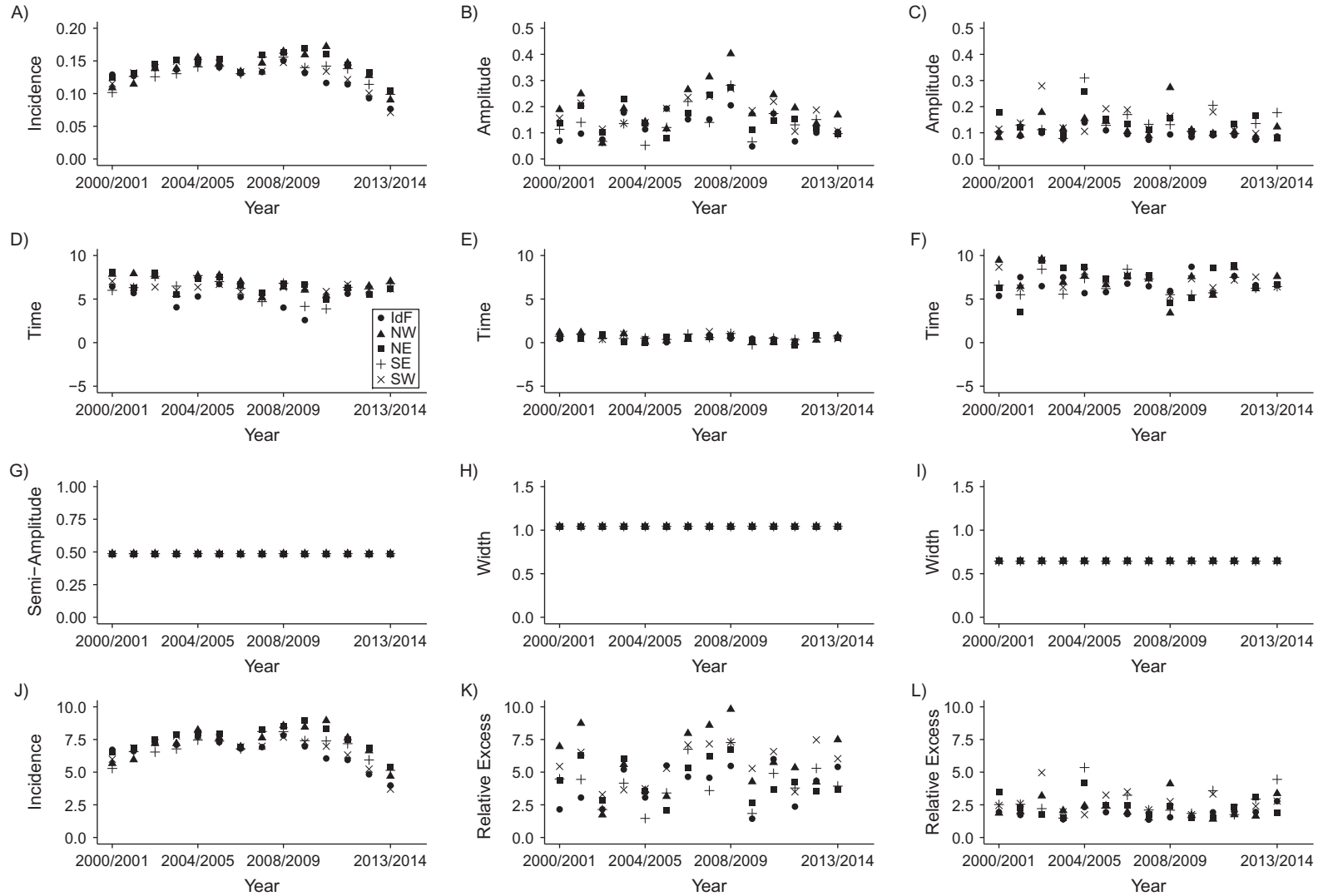


**Figure 4.** Invasive pneumococcal disease (IPD) seasonal waveforms, France, 2000–2014. The parameter estimates are presented every year (x-axis) in every region (symbol). The y-axis values differ for each panel. Left-hand column (A, D, G, J): seasonal baseline waveforms. A) Average incidence ( $\mu$ , cases per week per 100,000); D) time ( $\phi_0$ , week); G) relative semi-amplitude ( $A_0$ , dimensionless); J) annual average incidence ( $n_w \mu$ , cases per year per 100,000). Middle column (B, E, H, K): peak 1 waveforms. B) Amplitude ( $A_1$ , per week per 100,000); E) time ( $\phi_1$ , week); H) width ( $\sigma_1$ , weeks); K) relative excess of cases ( $2A_1\sigma_1/(n_w \mu)$ , %). Right-hand column (C, F, I, L): peak 2 waveforms. C) Amplitude ( $A_2$ , per week per 100,000); F) time ( $\phi_2$ , week); I) width ( $\sigma_2$ , weeks); L) relative excess of cases ( $2A_2\sigma_2/(n_w \mu)$ , %). Abbreviations: IdF, Île-de-France; NW, Northwest; NE, Northeast; SE, Southeast; SW, Southwest.

**Table 1.** Estimated Correlations Between Seasonal Waveforms for Influenza-Like Illness and Invasive Pneumococcal Disease, France, 2000–2014

Peak Comparison	Region-Years		Correlation <sup>a</sup> in Total Cases <i>E</i>		Correlation <sup>a</sup> in Peak Time, $\phi$		Difference of Peak Times IPD–ILI, weeks	
	Description	No.	Value	95% CI <sup>b</sup>	Value	95% CI <sup>b</sup>	Value	95% CI
ILI–IPD peak 1	All included	70	0.14	–0.23, 0.44	–0.09	–0.53, 0.35	–3.8	–5.5, –1.7
ILI–IPD peak 2	All included	70	0.20	–0.05, 0.46	0.32	0.01, 0.55	2.7	1.0, 4.7
ILI–IPD peak 2	Years 2003/2004 and 2009/2010 excluded	60	0.31	0.03, 0.56	0.42	0.04, 0.66	1.3	0.6, 2.0

Abbreviations: CI, confidence interval; ILI, influenza-like illness; IPD, invasive pneumococcal disease.

<sup>a</sup> Spearman correlation coefficients.

<sup>b</sup> 95% CI calculated using a block bootstrap, as described in the Methods section.

0.75) in 60 region-years with ILI peak during week 0–10). Therefore, the direct model and the seasonal waveforms comparison provided broadly comparable results, even though the associations estimated by the latter method were smaller.

## DISCUSSION

We examined the seasonalities of ILIs and IPDs based on highly resolved incidence data in France. To do so, we developed a new method to estimate summary statistics of seasonal shape (or seasonal waveforms) via nonlinear mixed-effects models. The method is well-suited to the analysis of spatially or temporally grouped data, which are common in epidemiology. It is also easily applicable, if an adequate functional form exists to model the disease considered. Using this method, we found high ILI-seasonality variability, with marked fluctuations of peak amplitude and peak time. In contrast, IPD seasonality was best modeled by a markedly regular, almost periodic seasonal baseline, punctuated by 2 winter peaks. Comparing the seasonal waveforms of ILI and IPD peaks, we found indication of a small, positive correlation.

As previously noted in epidemiologic studies (10, 14, 16–18, 47), our results support the observation that the amplitude and time of ILI epidemics vary substantially over time. Although the mechanisms causing ILI seasonality remain incompletely understood (23), this variability could reflect between-season influenza-virus antigenic changes (48), variations of weather conditions, or chance events caused by the random introduction of infected individuals into the population every year. In contrast, the epidemic duration was more conserved than peak times and amplitudes in our data; our average estimate of 12.5 weeks agrees with previous European and American studies, which relied on definitions of epidemic thresholds (14, 17, 47). Our results also indicate high synchrony of peak times across regions (calculated as the maximal difference of peaks times between regions each year): On average, ILI took 2.0 (range, 0.7–4.1) weeks to spread across continental France (roughly  $5 \times 10^5$  km<sup>2</sup>). In light of that relatively small area, this finding was expected and agrees with the spatial correlation structure inferred for influenza (49).

In accordance with earlier studies (10, 14, 15, 19), we found a remarkably stable IPD seasonal baseline, with large-amplitude

(approximately 50% relative to the annual average) oscillations peaking around week 6 (early February) or, equivalently, reaching a nadir during week 32 (early August). It should be kept in mind that these results are contingent on the choice of a sine wave to model IPD seasonal baseline, an ad hoc but common functional form used in numerous studies (8, 10, 14, 15, 31). Despite repeated observations of this seasonal pattern, its causes remain poorly understood (24). Experimental evidence shows that temperature and humidity affect influenza virus transmission and survival (21, 22), but, to our knowledge, such evidence is lacking for pneumococcus. The roles of these two climatic variables in shaping IPD seasonality have been assessed in several ecological studies, with discordant results (10, 11, 29, 50). Alternatively, it has been proposed that IPD seasonality is driven by variations of host susceptibility to infection caused by seasonal photoperiod changes (7, 19), a hypothesis supported by a few experimental (51–53) and ecological studies (10, 11, 15). Although beyond the scope of this study, the IPD-climate association could be studied by applying our method to calculate the seasonal waveforms of candidate weather parameters.

In addition to the seasonal baseline, we detected a first IPD winter peak constantly occurring at the end of every calendar year, of very regular duration but more variable amplitude. That peak was also observed previously (8, 11, 14, 31, 54), including an American study whose authors advanced that it represented a calendar effect, attributable to family gatherings during Christmas holidays (19). Notably, that peak concerned only adults aged  $\geq 18$  years, while an earlier rise of juvenile cases was seen in autumn (19). Because we found no definite spatial structure in the region-level data, we examined the age-specific IPD seasonality using country-level incidence data (Web Figure 10). In keeping with previous studies (19, 55, 56), we observed a distinct autumn peak in children  $< 5$  years. Another peak also occurred at the end of the year for that age group, but was less pronounced and arose earlier than that of older individuals, particularly those  $\geq 60$  years. This lag suggests transmission from young children to older persons, consistent with a calendar effect during Christmas holidays (57). Alternatively, this peak might be associated with the respiratory syncytial virus (RSV), which peaks earlier and less variably than influenza (58, 59). Transmission models integrating seasonal contact-rate changes will be useful to dissect these different hypotheses.



Compared with IPD winter peak 1, peak 2 had a more variable time and had less impact, except for a few region-years. Because peak 2 overlapped with the period of ILI circulation, we postulated that it might be associated with ILIs, but we found only a small association. Notably, in keeping with previous evidence that the 2009 A(H1N1) pandemic had low impact in most age groups in France (36), that association remained small during 2009/2010 (Web Figure 9). Although this small correspondence indicates little association at the population level, it may still be consistent with a strong interaction at the individual level. Indeed, strong experimental evidence from animal models indicates that influenza-virus infection facilitates pneumococcal acquisition, transmission, and disease (26, 27). Recent results from population-based mechanistic models can help explain this discrepancy (60, 61). Specifically, Shrestha et al. demonstrated that, despite strong interaction at the individual level, large variations of ILI-peak amplitude resulted in much lower variations of pneumococcal pneumonia peaks at the population level (61). That said, the associations estimated by the seasonal waveforms comparison were small, a finding also borne out by the direct regression models. Consequently, our results imply only a modest population-level impact of ILIs on IPDs (11, 14).

With few exceptions (28, 30), the ILI–pneumococcal infection association was estimated using standard regression models for count data (8, 11, 14, 29, 31). In comparison, our method also aims at characterizing seasonality, but several limitations are worth noting with regard to quantifying that association. First, our method requires an appropriate empirical model to represent the dynamics of the cocirculating pathogens, therefore limiting its applicability to those with unambiguous seasonality. Furthermore, it effectively compresses the whole body of data into a few summary statistics, a procedure that may cause some signal of association to be lost. Indeed, we found that, while our method and direct regression provided broadly comparable results, the associations estimated by the latter were moderately larger. Acknowledging the potential shortcomings of any statistical technique in ecological studies (62), we recommend using and comparing a variety of methods to examine the association between ILIs and pneumococcus.

Our study has several limitations. First, the ILI incidence data were not laboratory-confirmed and therefore might not be specific to influenza, which other respiratory viruses can be confused with clinically (59). Nevertheless, we think that concern should be limited because of the very specific ILI case definition; indeed, ILI clinical data correlated well with laboratory-confirmed influenza in previous studies in France (36, 63). In Web Figure 11 and Web Table 8, we provide further evidence of this marked correlation by comparing the seasonal waveforms of ILI and flu-specific time series calculated during 2014/2015 and 2015/2016, the first 2 seasons of virological data collection in the *Sentinelles* network. Second, we only considered 2 IPD peaks during winter, although other peaks were evident in our data. Therefore, our model could be extended to assess the association of additional IPD peaks with other respiratory viruses. Third, the IPD analysis was not stratified by age, although previous studies indicated a possible age-specific association between pneumococcal diseases and respiratory viruses (11, 29, 31, 64, 65). However, we repeated our estimations in age groups 5–60 years and  $\geq 60$  years, and

found our main results to be robust (Web Table 9). Fourth, the IPD data were not stratified by serotype, even though one study found evidence that influenza affects pneumococcal pneumonia in a serotype-specific manner (66). Another study's results showed, however, that IPD seasonality did not change after the introduction of the pneumococcal conjugate vaccine, despite substantial serotype replacement (14)—a finding confirmed by our results.

In conclusion, we provided a comprehensive picture of ILI and IPD seasonalities based on detailed incidence data. Our findings add knowledge to the epidemiology of these two diseases and may help generate new hypotheses about their seasonal dynamics. Such comparative studies are essential to better understand the still enigmatic seasonal patterns of ILIs and IPDs.

## ACKNOWLEDGMENTS

Author affiliations: Biostatistics, Biomathematics, Pharmacoepidemiology and Infectious Diseases (B2PHI), Institut national de la santé et de la recherche médicale (Inserm), Université de Versailles-Saint-Quentin-en-Yvelines (UVSQ), Institut Pasteur, Université Paris-Saclay, Paris, France (Matthieu Domenech de Cellès, Hélène Arduin, Didier Guillemot, Laurence Watier, Lulla Opatowski); Assistance publique–Hôpitaux de Paris (AP-HP), Hôpital Européen Georges-Pompidou, Laboratoire de Bactériologie, Paris, France (Emmanuelle Varon); Centre National de Référence des Pneumocoques, Paris, France (Emmanuelle Varon); Sorbonne Universités, Université Pierre et Marie Curie–UPMC (Paris 6), Inserm, Institut Pierre Louis d'épidémiologie et de Santé Publique (IPLESP unité mixte de recherche en santé [UMRS] 1136), Paris, France (Cécile Souty, Pierre-Yves Boëlle); Santé publique France, Saint-Maurice, France (Daniel Lévy-Bruhl); Institut Pasteur, Unité de Génétique Moléculaire des Virus à ARN, Département de Virologie, Paris, France (Sylvie van der Werf); Centre national de la recherche scientifique (CNRS), unité mixte de recherche (UMR) 3569, Paris, France (Sylvie van der Verf); Université Paris Diderot, Sorbonne Paris Cité, Unité de Génétique Moléculaire des Virus à ARN, Paris, France (Sylvie van der Werf); and Open Rome (Organize and Promote Epidemiological Network), Paris, France (Jean-Claude Soulayr).

This work was supported directly by internal resources of the French National Institute for Health and Medical Research, the Institut Pasteur, and the University of Versailles–Saint-Quentin-en-Yvelines. This study received funding from the Île-de-France region (Domaine d'intérêt majeur Malinf) and from the French Government's "Investissement d'Avenir" program, Laboratoire d'Excellence "Integrative Biology of Emerging Infectious Diseases" (grant ANR-10-LABX-62-IBEID). Data and R code are available from the Dryad Digital Repository: doi:10.5061/dryad.tg5qb.

We thank Dr. Anne Mosnier, Dr. Isabelle Daviaud, and Dr. Pejman Rohani for helpful comments on the manuscript. We thank Dr. Scarlett Georges for extracting the IPD data.

Conflicts of interest: E.V. received grants from French Institute for Public Health Surveillance during the conduct of

the study, and received grants from Pfizer and personal fees from Pfizer outside the submitted work. S.W. has received consulting fees from Danone through her research unit. The other authors report no conflicts.

## REFERENCES

- Altizer S, Dobson A, Hosseini P, et al. Seasonality and the dynamics of infectious diseases. *Ecol Lett*. 2006;9(4):467–484.
- Fisman DN. Seasonality of infectious diseases. *Annu Rev Public Health*. 2007;28:127–143.
- Grassly NC, Fraser C. Seasonal infectious disease epidemiology. *Proc Biol Sci*. 2006;273(1600):2541–2550.
- Nair H, Brooks WA, Katz M, et al. Global burden of respiratory infections due to seasonal influenza in young children: a systematic review and meta-analysis. *Lancet*. 2011;378(9807):1917–1930.
- Bogaert D, De Groot R, Hermans PW. *Streptococcus pneumoniae* colonisation: the key to pneumococcal disease. *Lancet Infect Dis*. 2004;4(3):144–154.
- Simell B, Auranen K, Käyhty H, et al. The fundamental link between pneumococcal carriage and disease. *Expert Rev Vaccines*. 2012;11(7):841–855.
- Dowell SF. Seasonal variation in host susceptibility and cycles of certain infectious diseases. *Emerg Infect Dis*. 2001;7(3):369–374.
- Grabowska K, Högberg L, Penttinen P, et al. Occurrence of invasive pneumococcal disease and number of excess cases due to influenza. *BMC Infect Dis*. 2006;6:58.
- Jansen AG, Sanders EA, VAN DER Ende A, et al. Invasive pneumococcal and meningococcal disease: association with influenza virus and respiratory syncytial virus activity? *Epidemiol Infect*. 2008;136(11):1448–1454.
- Kuster SP, Tuite AR, Kwong JC, et al. Evaluation of coseasonality of influenza and invasive pneumococcal disease: results from prospective surveillance. *PLoS Med*. 2011;8(6):e1001042.
- Nicoli EJ, Trotter CL, Turner KM, et al. Influenza and RSV make a modest contribution to invasive pneumococcal disease incidence in the UK. *J Infect*. 2013;66(6):512–520.
- Opatowski L, Varon E, Dupont C, et al. Assessing pneumococcal meningitis association with viral respiratory infections and antibiotics: insights from statistical and mathematical models. *Proc Biol Sci*. 2013;280(1764):20130519.
- Talbot TR, Poehling KA, Hartert TV, et al. Seasonality of invasive pneumococcal disease: temporal relation to documented influenza and respiratory syncytial viral circulation. *Am J Med*. 2005;118(3):285–291.
- Walter ND, Taylor TH, Shay DK, et al. Influenza circulation and the burden of invasive pneumococcal pneumonia during a non-pandemic period in the United States. *Clin Infect Dis*. 2010;50(2):175–183.
- White AN, Ng V, Spain CV, et al. Let the sun shine in: effects of ultraviolet radiation on invasive pneumococcal disease risk in Philadelphia, Pennsylvania. *BMC Infect Dis*. 2009;9:196.
- Fleming DM, Elliot AJ. Lessons from 40 years' surveillance of influenza in England and Wales. *Epidemiol Infect*. 2008;136(7):866–875.
- Fleming DM, Zambon M, Bartelds AI, et al. The duration and magnitude of influenza epidemics: a study of surveillance data from sentinel general practices in England, Wales and the Netherlands. *Eur J Epidemiol*. 1999;15(5):467–473.
- te Beest DE, van Boven M, Hooiveld M, et al. Driving factors of influenza transmission in the Netherlands. *Am J Epidemiol*. 2013;178(9):1469–1477.
- Dowell SF, Whitney CG, Wright C, et al. Seasonal patterns of invasive pneumococcal disease. *Emerg Infect Dis*. 2003;9(5):573–579.
- Cauchemez S, Valleron AJ, Boëlle PY, et al. Estimating the impact of school closure on influenza transmission from sentinel data. *Nature*. 2008;452(7188):750–754.
- Lowen AC, Mubareka S, Steel J, et al. Influenza virus transmission is dependent on relative humidity and temperature. *PLoS Pathog*. 2007;3(10):1470–1476.
- Shaman J, Kohn M. Absolute humidity modulates influenza survival, transmission, and seasonality. *Proc Natl Acad Sci USA*. 2009;106(9):3243–3248.
- Lipsitch M, Viboud C. Influenza seasonality: lifting the fog. *Proc Natl Acad Sci USA*. 2009;106(10):3645–3646.
- van Hoek AJ, Miller E. Editorial commentary: seasonal changes in pneumococcal disease – still much of an enigma. *Clin Infect Dis*. 2014;58(2):195–196.
- McCullers JA. Insights into the interaction between influenza virus and pneumococcus. *Clin Microbiol Rev*. 2006;19(3):571–582.
- Diavatopoulos DA, Short KR, Price JT, et al. Influenza A virus facilitates *Streptococcus pneumoniae* transmission and disease. *FASEB J*. 2010;24(6):1789–1798.
- McCullers JA, McAuley JL, Browall S, et al. Influenza enhances susceptibility to natural acquisition of and disease due to *Streptococcus pneumoniae* in ferrets. *J Infect Dis*. 2010;202(8):1287–1295.
- Hendriks W, Boshuizen H, Dekkers A, et al. Temporal cross-correlation between influenza-like illnesses and invasive pneumococcal disease in the Netherlands. *Influenza Other Respir Viruses*. 2017;11(2):130–137.
- Murdoch DR, Jennings LC. Association of respiratory virus activity and environmental factors with the incidence of invasive pneumococcal disease. *J Infect*. 2009;58(1):37–46.
- Toschke AM, Arenz S, von Kries R, et al. No temporal association between influenza outbreaks and invasive pneumococcal infections. *Arch Dis Child*. 2008;93(3):218–220.
- Weinberger DM, Harboe ZB, Viboud C, et al. Pneumococcal disease seasonality: incidence, severity and the role of influenza activity. *Eur Respir J*. 2014;43(3):833–841.
- Flahault A, Blanchon T, Dorléans Y, et al. Virtual surveillance of communicable diseases: a 20-year experience in France. *Stat Methods Med Res*. 2006;15(5):413–421.
- Valleron AJ, Bouvet E, Garnerin P, et al. A computer network for the surveillance of communicable diseases: the French experiment. *Am J Public Health* 1986;76(11):1289–1292.
- Turbelin C, Souty C, Pelat C, et al. Age distribution of influenza like illness cases during post-pandemic A(H3N2): comparison with the twelve previous seasons, in France. *PLoS One*. 2013;8(6):e65919.
- Costagliola D, Flahault A, Galinec D, et al. A routine tool for detection and assessment of epidemics of influenza-like syndromes in France. *Am J Public Health*. 1991;81(1):97–99.
- Lemaitre M, Carrat F, Rey G, et al. Mortality burden of the 2009 A/H1N1 influenza pandemic in France: comparison to seasonal influenza and the A/H3N2 pandemic. *PLoS One*. 2012;7(9):e45051.
- Lepoutre A, Varon E, Georges S, et al. Impact of the pneumococcal conjugate vaccines on invasive pneumococcal disease in France, 2001–2012. *Vaccine*. 2015;33(2):359–366.
- Lepoutre A, Varon E, Georges S, et al. Impact of infant pneumococcal vaccination on invasive pneumococcal diseases in France, 2001–2006. *Euro Surveill*. 2008;13(35):18962.

39. French National Institute of Statistics and Economic Studies. Demographic estimates. <https://www.insee.fr/en/statistiques/2418112>. Accessed June 1, 2016.
40. Keeling MJ, Rohani P. *Modeling Infectious Diseases in Humans and Animals*. Princeton, NJ: Princeton University Press; 2008.
41. Kermack WO, McKendrick AG. A contribution to the mathematical theory of epidemics. *Proc R Soc Lond A Math Phys Eng Sci.* 1927;115(772):700–721.
42. Pinheiro JC, Bates DM. *Mixed-Effects Models in S and S-PLUS*. New York, NY: Springer; 2000.
43. Pinheiro J, Bates D, DebRoy S, et al. *nlme 3.1.128: Linear and Nonlinear Mixed Effects Models*. 2016. <https://CRAN.R-project.org/package=nlme>. Accessed January 22, 2017.
44. R Core Team. *R: A Language and Environment for Statistical Computing*. Vienna, Austria: R Foundation for Statistical Computing; 2016. <https://www.R-project.org/>.
45. Alari A, Chaussade H, Domenech de Cellès M, et al. Impact of pneumococcal conjugate vaccines on pneumococcal meningitis cases in France between 2001 and 2014: a time series analysis. *BMC Med.* 2016;14(1):211.
46. Domenech de Cellès M, Pons-Salort M, Varon E, et al. Interaction of vaccination and reduction of antibiotic use drives unexpected increase of pneumococcal meningitis. *Sci Rep.* 2015;5:11293.
47. Viboud C, Boëlle PY, Pakdaman K, et al. Influenza epidemics in the United States, France, and Australia, 1972–1997. *Emerg Infect Dis.* 2004;10(1):32–39.
48. De Jong JC, Rimmelzwaan GF, Fouchier RA, et al. Influenza virus: a master of metamorphosis. *J Infect.* 2000;40(3):218–228.
49. Viboud C, Bjørnstad ON, Smith DL, et al. Synchrony, waves, and spatial hierarchies in the spread of influenza. *Science.* 2006;312(5772):447–451.
50. Tvedebrink T, Lundbye-Christensen S, Thomsen RW, et al. Seasonal changes in climatic parameters and their relationship with the incidence of pneumococcal bacteraemia in Denmark. *Clin Microbiol Infect.* 2008;14(12):1183–1186.
51. Feigin RD, San Joaquin VH, Haymond MW, et al. Daily periodicity of susceptibility of mice to pneumococcal infection. *Nature.* 1969;224(5217):379–380.
52. Shackelford PG, Feigin RD. Periodicity of susceptibility to pneumococcal infection: influence of light and adrenocortical secretions. *Science.* 1973;182(4109):285–287.
53. Wongwiwat M, Sukapanit S, Triyanond C, et al. Circadian rhythm of the resistance of mice to acute pneumococcal infection. *Infect Immun.* 1972;5(4):442–448.
54. Kim PE, Musher DM, Glezen WP, et al. Association of invasive pneumococcal disease with season, atmospheric conditions, air pollution, and the isolation of respiratory viruses. *Clin Infect Dis.* 1996;22(1):100–106.
55. Dagan R, Engelhard D, Piccard E, et al. Epidemiology of invasive childhood pneumococcal infections in Israel. The Israeli Pediatric Bacteremia and Meningitis Group. *JAMA.* 1992;268(23):3328–3332.
56. Eskola J, Takala AK, Kela E, et al. Epidemiology of invasive pneumococcal infections in children in Finland. *JAMA.* 1992;268(23):3323–3327.
57. Walter ND, Taylor TH Jr, Dowell SF, et al. Holiday spikes in pneumococcal disease among older adults. *N Engl J Med.* 2009;361(26):2584–2585.
58. Lina B, Valette M, Foray S, et al. Surveillance of community-acquired viral infections due to respiratory viruses in Rhone-Alpes (France) during winter 1994 to 1995. *J Clin Microbiol.* 1996;34(12):3007–3011.
59. Zambon MC, Stockton JD, Clewley JP, et al. Contribution of influenza and respiratory syncytial virus to community cases of influenza-like illness: an observational study. *Lancet.* 2001;358(9291):1410–1416.
60. Shrestha S, Foxman B, Berus J, et al. The role of influenza in the epidemiology of pneumonia. *Sci Rep.* 2015;5:15314.
61. Shrestha S, Foxman B, Weinberger DM, et al. Identifying the interaction between influenza and pneumococcal pneumonia using incidence data. *Sci Transl Med.* 2013;5(191):191ra184.
62. Gilca R, De Serres G, Skowronski D, et al. The need for validation of statistical methods for estimating respiratory virus-attributable hospitalization. *Am J Epidemiol.* 2009;170(7):925–936.
63. Souty C, Blanchon T, Bonmarin I, et al. Early estimates of 2014/15 seasonal influenza vaccine effectiveness in preventing influenza-like illness in general practice using the screening method in France. *Hum Vaccin Immunother.* 2015;11(7):1621–1625.
64. Weinberger DM, Klugman KP, Steiner CA, et al. Association between respiratory syncytial virus activity and pneumococcal disease in infants: a time series analysis of US hospitalization data. *PLoS Med.* 2015;12(1):e1001776.
65. Weinberger DM, Simonsen L, Jordan R, et al. Impact of the 2009 influenza pandemic on pneumococcal pneumonia hospitalizations in the United States. *J Infect Dis.* 2012;205(3):458–465.
66. Weinberger DM, Harboe ZB, Viboud C, et al. Serotype-specific effect of influenza on adult invasive pneumococcal pneumonia. *J Infect Dis.* 2013;208(8):1274–1280.